

# A Structure–Property Study of IPDI-Based Polyurethane Anionomers

D. J. HOURSTON,<sup>1</sup> G. WILLIAMS,<sup>1</sup> R. SATGURU,<sup>2</sup> J. D. PADGET,<sup>2</sup> D. PEARS<sup>2</sup>

<sup>1</sup> Institute of Polymer Technology and Materials Engineering, Loughborough University, Loughborough, Leicestershire, LE11 3TU, United Kingdom

<sup>2</sup> Zeneca Resins, Research & Technology Department, P.O. Box 8, The Heath, Runcorn, Cheshire, WA7 4QD, United Kingdom

Received 4 June 1997; accepted 9 August 1997

**ABSTRACT:** Polyurethane (PU) anionomers were prepared as aqueous dispersions and as solutions in tetrahydrofuran or absolute ethanol using dimethylol propionic acid (DMPA) as the stabilizing moiety, isophorone diisocyanate, polytetrahydrofuran, and cyclohexane dimethanol. The structure–property relationships were investigated for these PUs, cast as films, at similar and differing chain-extension levels. Comparisons were made with respect to the mechanical and viscoelastic properties and solvent resistance. Finally, the consequences of DMPA incorporation into the PU backbone were determined for two solvent-borne compositions of similar structure with and without DMPA. Dynamic mechanical thermal analysis, tensiometry, solvent spot tests, and swelling studies were employed for the characterization of the materials. © 1998 John Wiley & Sons, Inc. *J Appl Polym Sci* **67**: 1437–1448, 1998

**Key words:** ionomer; polyurethane; structure–property relations

## INTRODUCTION

In the past, conventional polyurethane (PU) coatings contained significant amounts of organic solvents and free isocyanate.<sup>1</sup> Increasing concern over environmental pollution and health and safety risks<sup>2</sup> led to the development of water-borne PU formulations. In contrast to the solvent-borne coatings, where the PU formed a solution in a solvent, the water-borne PUs exist as aqueous dispersions, and these have recently found use in coatings for textiles and leathers. However, it is important to note that, in general, solvent-borne urethanes are used as two-pack systems, i.e., in the presence of a crosslinking agent and not on their own. Water-borne ure-

thane dispersions, however, if properly designed, can be used on their own in various coating applications. A water-borne PU dispersion can be defined as a binary colloidal system in which PU particles are dispersed in a continuous aqueous medium.<sup>3</sup> To render the PU polymer dispersible in water,<sup>4</sup> PUs should contain ionic and/or nonionic hydrophilic segments in their structure. This led to the development of PU ionomers<sup>5–7</sup> where the PUs possess pendant acid groups (anionomer) or tertiary amine groups (cationomer) incorporated into their backbones. These groups are neutralized to form internal salts prior to dispersion. A typical reaction scheme is shown in Figure 1. Nonionic PUs are also available where nonionic stabilizing moieties are employed. The advantages and disadvantages of ionic and nonionic type PUs are well documented.<sup>8,9</sup> The PU is usually prepared as a low molecular weight NCO-endcapped prepolymer for ease of dispersion. Then, diamines are

---

Correspondence to: D. J. Hourston.  
Contract grant sponsor: Zeneca Resins.



**Table II** Characterization of a Water-borne and Solvent-borne Sample of Similar Composition

Specification	AQ1 <sup>a</sup>	SOL1 <sup>b</sup>
Viscosity (Pa s)	0.38	0.22
DMTA		
$T_{gs}$ (°C)	-52	-41
$T_{gh}$ (°C)	78	35
Tensile strength (MPa)	50.0	8.9
Initial modulus (MPa)	22.4	9.0
Elongation at break (%)	314	91
Overall solvent spot <sup>c</sup>	33	14
Swelling in		
2-Butanone	133	Dissolved
2-Propanol	231	Dissolved
Water	56	25
DMF	Dissolved	Dissolved
Xylene	84	182

<sup>a</sup> Aqueous dispersion at 98% chain extension.

<sup>b</sup> PU solution in THF at 120% chain extension.

<sup>c</sup> Overall solvent spot test results are the total score out of a maximum of 70 for the film in various solvents.

## EXPERIMENTAL

### Materials

Polytetrahydrofuran (PTHF) ( $M_n = 1000$ , Aldrich) was dried at 0.1 mmHg and 80°C for 3 h before use. Extrapure grades of DMPA (Aldrich), triethylamine (TEA, Aldrich), *N*-methyl-2-pyrrolidone (NMP, Aldrich), cyclohexane dimethanol (CHDM, Aldrich), and isophorone diisocyanate (IPDI, Aldrich) were used without further purification. Dibutyl tin dilaurate (DBTDL, Aldrich), used to catalyze the reaction, and the chain extender, hydrazine monohydrate (Aldrich), were used as received. Extrapure grade tetrahydrofuran (THF) and absolute ethanol (EtOH) were used for the solvent-borne systems.

### Procedure

A series of water-borne and solvent-borne PUs were prepared. Their specifications are presented in Table I. The prepolymer reaction apparatus consisted of a 250 mL flange flask and lid, nitrogen bubbler and inlet, thermometer, and stirrer and paddle. The reaction temperature was controlled using a constant-temperature oil bath. The CHDM, PTHF, and the DMPA as a solution in NMP were weighed out into a clean, dry flask. The contents were then heated to 50°C, with stirring to homogenize. At

50°C, the IPDI and the first portion of catalyst, DBTDL, were added. The reaction temperature was increased to 95°C, where it was maintained for 1 h. A further portion of the catalyst was then added and the reaction continued at 95°C for a further hour. The temperature was then lowered to 70°C and the %NCO value was determined using the standard dibutylamine back titration method.<sup>24</sup> On achieving a %NCO value close to that of the theoretical value, preneutralization of the carboxylic acid groups was carried out by addition of the TEA. The temperature was maintained at 70°C for 30 min, at which point a prepolymer had now been prepared ready for dispersion. Dispersion was carried out by adding the prepolymer, in a controlled manner, to a three-necked round-bottom flask fitted with an addition funnel, stirrer, and condenser. The flask contained water or THF, and the chain extender, hydrazine monohydrate. Dispersion was carried out over a 40-min time interval to ensure that the dispersion temperature did not exceed 40°C. The dispersion was then allowed to stir for further 30 min. The dispersions were prepared at 35 wt % solids and the solutions in THF at 20 wt % solids.

Films from the samples were prepared by pouring the dispersion/solution into an aluminum mold coated with a release agent. The films were allowed to dry at room temperature for 2 days. The residual solvent was removed by placing the films overnight into a vacuum oven at 20°C. These films were then used for DMTA, DSC, swelling, tensile testing, and wide-angle X-ray diffraction (WAXD) analyses.

### Characterization

#### Photon Correlation Spectroscopy

Particle-size analysis was determined for the dispersions by light scattering using a Malvern Autosizer Model Iic.

#### Tensile Testing

Tensile properties were measured at room temperature using a J. J. Lloyd tensometer following ASTM D-412 specifications. A crosshead speed of 50 mm/min was used throughout these investigations.

#### Differential Scanning Calorimetry

Differential scanning calorimetry (DSC) thermograms, under nitrogen and over the temperature

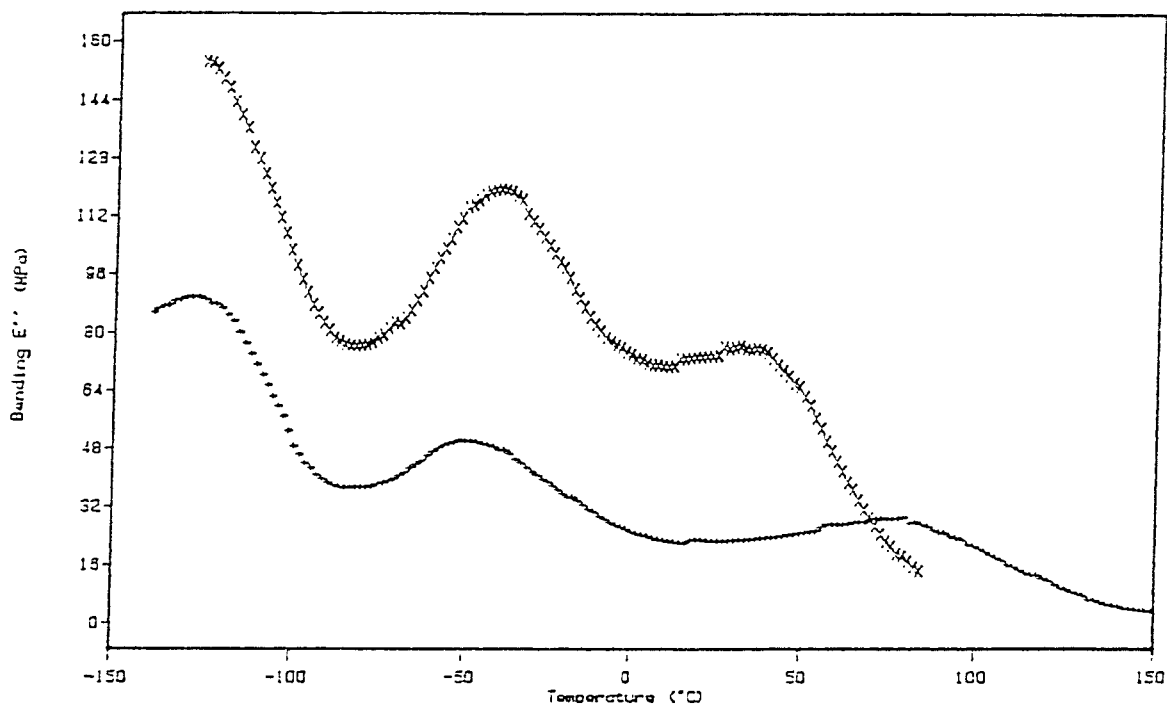


**Figure 2** Loss modulus versus temperature plot of the (+) water-borne AQ1 (98%) and (x) solvent-borne SOL1 (120%) samples of similar composition, but differing level of chain extension. Conducted in the bending mode.

range  $-100$  to  $150^{\circ}\text{C}$ , were obtained using a DuPont 910 apparatus at a heating rate of  $20^{\circ}\text{C}/\text{min}$ .

#### **Gel Permeation Chromatography (GPC)**

The average molecular weights,  $M_n$  and  $M_w$ , were determined by use of a Polymer Laboratories GPC fitted with a Knauer HPLC pump and a differential refractometer. A PLgel  $10\text{-}\mu\text{m}$  mixed-bed B column was employed for the analysis. THF was used as the continuous phase and was pumped through the column at a flow rate of  $1.0\text{ mL}/\text{min}$ .

#### **Dynamic Mechanical Thermal Analysis**

DMTA analyses were undertaken over the temperature range  $-100$  to  $150^{\circ}\text{C}$  using a Polymer Laboratories DMTA (Mark II) at a frequency of  $10\text{ Hz}$ , a strain amplitude setting of  $\times 4$ , and a heating rate of  $4^{\circ}\text{C}/\text{min}$ . Both single cantilever clamping and shear mode systems were used.

#### **Wide-Angle X-ray Spectroscopy**

Wide-angle X-ray diffraction (WAXD) experiments were conducted using a Shimadzu Model XD-5 diffractometer operated at  $30\text{ kV}$  and  $20\text{ mA}$  over an angular range ( $2\theta$ ) of  $5^{\circ}$  to  $40^{\circ}$  at a

scan rate of  $4^{\circ}/\text{min}$ . The smoothing time constant was  $4\text{ s}$ .

#### **Infrared Spectroscopy**

Infrared (IR) analysis was carried out using a Unicam Mattson 3000 FTIR spectrophotometer.

#### **Swelling Studies**

To measure swelling in water, 2-butanone, 2-propanol (IPA), dimethylformamide (DMF), and xylene, films were immersed in each solvent for  $24\text{ h}$  at room temperature and the percentage swelling was determined by measuring the weight increase:

$$\% \text{ Swelling} = 100(W - W_0)/W_0$$

$W_0$  is the weight of the dried film and  $W$  is the weight of the film at equilibrium swelling.

#### **Solvent Spot Testing**

The solvent resistance of the films was determined by exposing the film to a solvent droplet (approximately  $1\text{ cm}$  in diameter) for  $1\text{ h}$  before removal of the droplet and inspection of the film. A

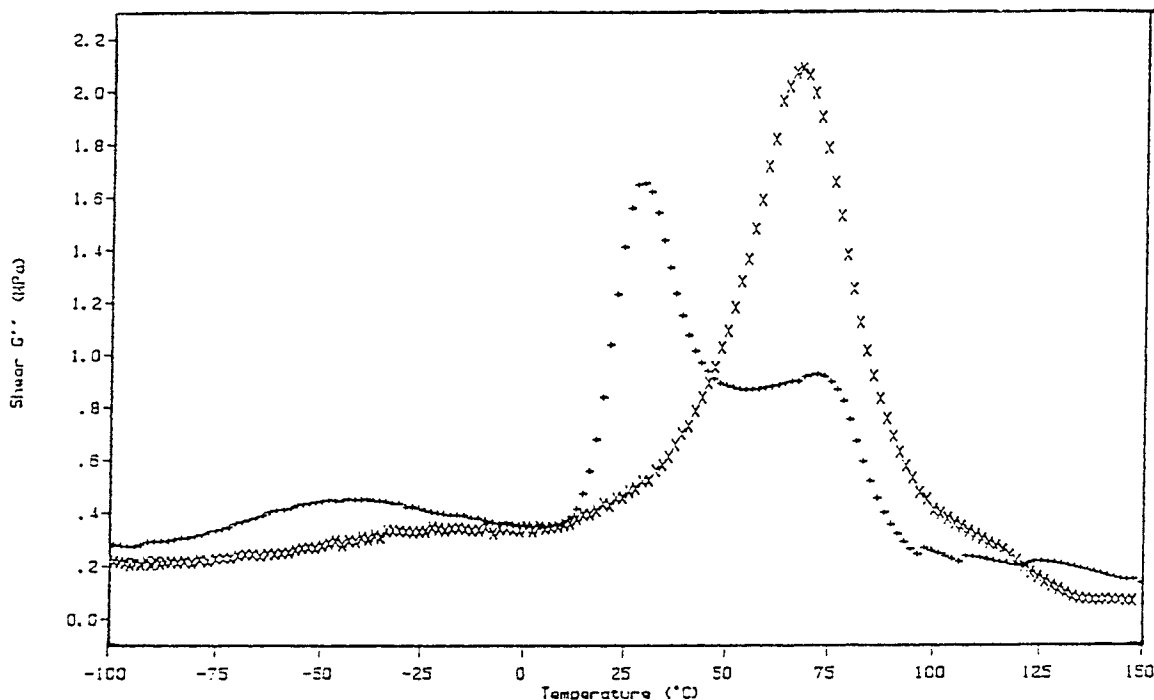


**Figure 3** Loss modulus versus temperature plots of the (+) water-borne AQ1 (98%) and (x) solvent-borne SOL1 (120%) samples of similar composition, but differing level of chain extension. Conducted in the shear mode.

subjective grading system of 0–10 was employed, where 0 is total dissolution of the film and 10 represents the total solvent resistance.

## RESULTS AND DISCUSSION

### Comparison of Water-Borne and Solvent-Borne Compositions

For this study, water-borne and solvent-borne samples were compared with respect to their mechanical properties and solvent resistance. The compositions of these samples, AQ1 and SOL1, are outlined in Table I. For all the samples listed in Table I, the prepolymer molecular weight, and, hence, viscosity, was minimized by adopting a NCO/OH ratio of 2. Lowering the viscosity of the prepolymer in this way made dispersion or solubilization significantly easier. The results obtained from the characterization of these two samples are shown in Table II.

The solvent-borne sample, SOL1, was prepared at 120% chain extension, and the water-borne sample, AQ1, at 98% chain extension. The chain-extension process relies on the reaction of the terminal isocyanate end groups in the prepolymer

with the  $\text{NH}_2$  groups of the diamine so that a high molecular weight is achieved. Therefore, for complete reaction and, hence, 100% chain extension to take place, a mol equivalent of the diamine is required. Hence, the percentage here refers to the degree of chain extension that takes place when the diamine is added. In this case, AQ1 has the greater molecular weight. Lower molecular weights will be achieved by adding more chain extender than is required for 100% chain extension as in the case for SOL1. Here, chain termination as well as chain extension takes place.

The solution viscosity for SOL1 was very similar to that of AQ1 even though their molecular weights will significantly differ. Increasing the molecular weight of SOL1 resulted in a gel-type structure being formed. In the solvent-borne sample, the PU actually dissolves in the solvent, making the solution viscosity-dependent upon the molecular weight at a fixed solids content. However, in water, the PU is insoluble and in the form of a dispersion of discrete particles. It is possible to form high molecular weight dispersions at relatively high solid contents because the dispersion viscosity is independent of the molecular weight. Hence, SOL1 consists of lower molecular weight

**Table III** Characterization of a Water-Borne and Solvent-Borne Sample of Similar Composition and Molecular Weight

Specification	AQ2 120% <sup>a</sup>	SOL1 120% <sup>a</sup>
Viscosity (Pa s)	0.29	0.22
DMTA		
$T_{gs}$ (°C)	-39	-41
$T_{gh}$ (°C)	29	35
Tensile strength (MPa)	11.9	8.9
Initial modulus (MPa)	7.8	9.0
Elongation at break (%)	169	91
Overall solvent spot	14	14
Swelling in		
2-Butanone	Dissolved	Dissolved
2-Propanol	Dissolved	Dissolved
Water	24	25
DMF	Dissolved	Dissolved
Xylene	199	182

<sup>a</sup> 120% chain extension based on moles of NCO groups in prepolymer.

PU chains in solution. The solution viscosity sets a practical limit to the level of chain extension that could be achieved for solvent-borne samples.

Each film was investigated by DMTA to deter-

mine the glass transition of the hard,  $T_{gh}$ , and soft,  $T_{gs}$ , domains. Using this technique, the degree of separation of the hard and soft domains within the PU structure was estimated. The DMTA traces for both samples are shown in Figure 2. The low-temperature transition at  $-121^{\circ}\text{C}$  is the result of the motion of small internal sections of the polymer chain, while the rest of the chain remains frozen. This is common for polyethers<sup>25</sup> containing at least four successive unsubstituted  $\text{CH}_2$  groups which undergo rotation in a crankshaft-type manner. However, the temperature and intensity of this peak was found to be independent of the structure of the rest of the PU and little information on phase separation was obtained. Extensive studies<sup>25-27</sup> of this transition have been carried out by several workers.

Examining the position of the transitions representing the soft and hard domains, an estimation of the degree of phase separation can be made. These transitions are clearly shown for both samples in Figure 2. These results suggest that more phase separation exists between the hard and soft domains in AQ1 (98%) than in SOL1 (120%). The soft-phase transition is a sensitive indication<sup>28</sup> of order within a PU. The closer the temperature at which this transition appears to that of the pure

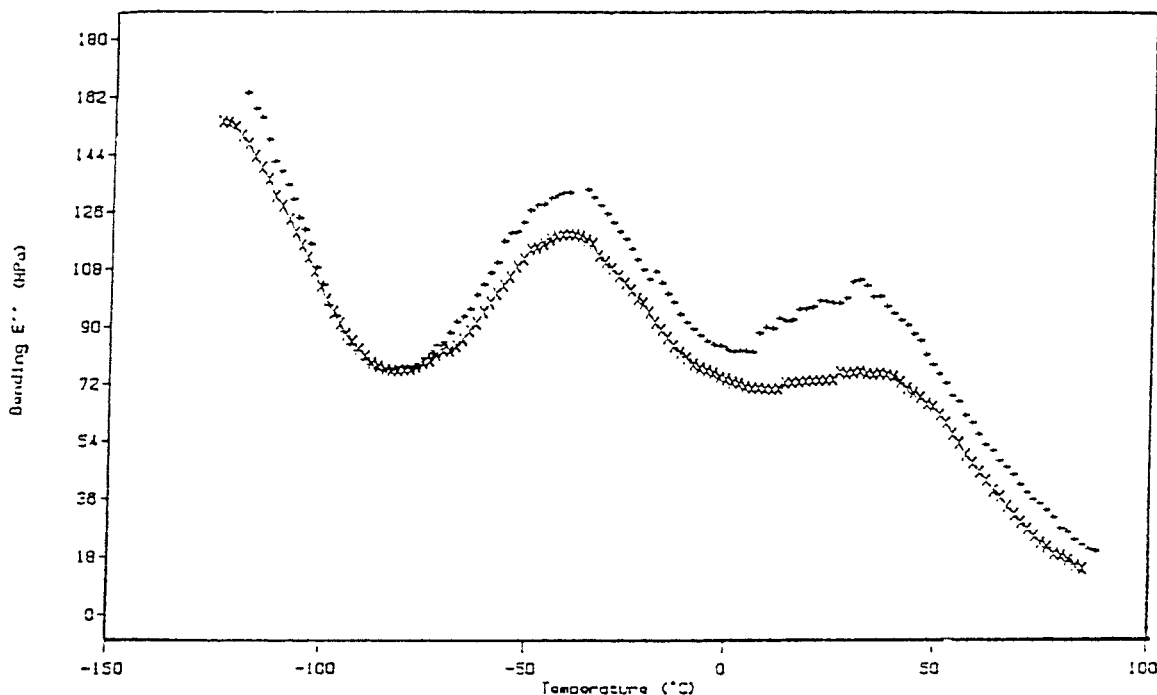


**Figure 4** Loss modulus versus temperature plots of the (+) water-borne AQ2 and (×) solvent-borne SOL1 samples of similar composition and level of chain extension. Conducted in the bending mode.

**Table IV Study of the Effect of the Level of Chain Extension on Sample Properties of Water-Borne and Solvent-Borne Compositions**

Specification	AQ1 98%	AQ2 120%	SOL1 120%	SOL2 150%
Overall solvent spot	33	14	14	14
Tensile strength (MPa)	50.0 (13.0) <sup>a</sup>	11.9 (0.2) <sup>a</sup>	8.9	6.3
Initial modulus (MPa)	22.4	7.8	9.0	7.5
Elongation (%)	314 (464) <sup>b</sup>	169 (761) <sup>b</sup>	91	63
DMTA $T_g$ (°C)	-52	-39	-41	-36
Particle size (nm)	57	81	N/A	N/A

<sup>a</sup> Tensile strengths from tests carried out at 80°C.

<sup>b</sup> Elongation from tests carried out at 80°C.

polyether  $T_g$  (PTHF -84°C) is indicative of the degree of hard-soft segment mixing. The differing structure of these two samples is the consequence of the increased number of hard-segment interactions resulting from the higher level of chain extension (lower molecular weight) and from urea-group formation. This favors the development of well-defined hard and soft domains in the water-borne sample. Knutson and Lyman<sup>29</sup> proposed that the morphology of a PU may be characterized by segments of polyether dispersed within the hard domains and/or by polyurethaneurea segments dispersed in the polyether matrix. They also described another alternative involving relatively pure polyurethaneurea and polyether domains separated by a rather broad interfacial zone. Shown in Figure 3 are the corresponding DMTA data obtained using the shear mode clamping system. In comparing the two spectra for the samples AQ1 and SOL1, there appears to be a clear indication that these have very different structures. For SOL1, there is one main peak shown for the loss modulus  $G''$  with the soft-segment  $T_g$  present as a minor transition. In contrast, three clear transitions are highlighted in the  $G''$  vs. temperature plot for AQ1. In comparing the high-temperature peak in both AQ1 (72°C) and SOL1 (68°C), there appears to be a shift to higher temperature as the level of chain extender was changed. This suggests increased ordering in the hard domains for AQ1. However, the peak at 29°C for AQ1, absent in SOL1, is very interesting. This peak is believed to be the consequence of the dissociation or rearrangement of interchain bonds. Hence, it is reasonable to say that these differences are the consequence of significant differences in hydrogen bonding within the samples. From an examination of the mechanical properties and sol-

vent resistance of the sample films, also shown in Table II, it is clear that significant differences occur as a result of their differing structure and molecular weight. The mechanical properties exhibited by each sample highlight the effect of hard- and soft-phase separation on the tensile strength, initial modulus, and elongation at break. AQ1 showed signs of stress whitening at high strain levels, a characteristic of PTHF-derived samples<sup>10</sup> where reversible stress-induced crystallization is possible. This phenomenon was not observed for SOL1 as a result of its significantly lower level of chain extension (120%) and less phase-separated structure.

Similar results were obtained from the study of the solvent resistance and swelling of the films. AQ1 (98%) was far more resistant to solvent attack than was the solvent-cast film. This, again, may be attributed to differences in molecular weight, resulting from differing levels of chain extension and also the phase structures of the two samples. Increasing molecular weight results in increasing numbers of chain entanglements which enhance the strength of the film. The two films also exhibited differing swelling behavior in the solvents as outlined in Table II.

The solvents used in this investigation are known to dissolve preferentially in the soft seg-

**Table V Average Molecular Weights for Samples AQ1 and AQ2 Determined by GPC**

Sample	Chain Extension (%)	$M_n$	$M_w$
AQ1	98	5600	366,000
AQ2	120	4100	24,200

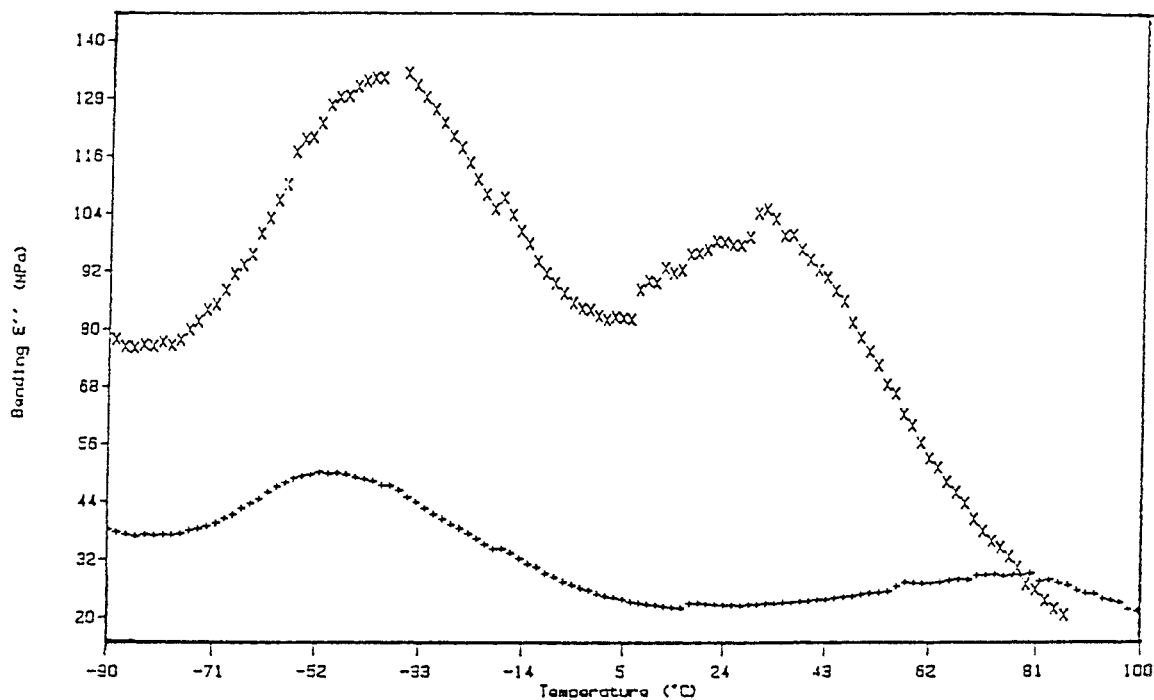


**Figure 5** Loss modulus versus temperature plots of the water-borne samples (+) AQ1, 98% chain extension, and (x) AQ2, 120% chain extension. Conducted in the bending mode.

ments of the PU, but are retarded<sup>30</sup> by the hard segments. Hence, the more mixed the hard and soft segments are, the less swelling will be experienced. Hence, swelling will increase if the phase separation is increased. The results in Table II suggest that SOL1 is more phase-separated than is AQ1. This was clearly not the case from the DMTA results, which showed that AQ1 is highly phase-separated compared to SOL1. Swelling may also have been retarded by the crystallinity of the soft segments in AQ1. However, this was discovered not to be the case from a study of the crystallinity of all these samples using DSC and WAXD. Hence, the differences observed for the swelling behavior of AQ1 and SOL1 must be a consequence of the differences in hydrogen bonding and ionic interactions involving the carboxylate groups. Also, the higher molecular weight of AQ1 results in increased chain entanglements. These entanglements restrict the motion of the polymer chains by acting as physical crosslinks. However, for SOL1, fewer of these physical crosslinks exist, and, hence, the SOL1 film is more easily swollen and the results in Table II indicate that in some instances complete dissolution of the film occurs.

The results from the characterization study of

two samples chain-extended to 120% are outlined in Table III. Examination of the mechanical properties of each indicate that there is now relatively little difference in their properties. The solvent spot tests also show a similar trend and there was very little difference in their swelling behavior. The DMTA traces for each sample are shown in Figure 4. This technique confirmed that when the samples are chain-extended to the same level the phase separation in each was almost identical. This was found to be true for both water-borne and solvent-borne samples.

#### Effect of Increasing Chain Extension on Sample Properties

It seems, from the results accumulated, that the degree of chain extension has a significant effect upon the properties exhibited by the sample, whether it be water-borne or solvent-borne. From Table IV, it can be seen that the "overextended" water-borne sample AQ2 has a considerably larger colloidal particle size. From the fact that the prepolymer synthesis is a step growth-type mechanism, it is inevitable that the polymer chains will be polydisperse in terms of molecular weight. As a consequence, it is possible that the



**Table VI Study of the Effect on Properties of Incorporating Ionic Groups into the PU Backbone**

Specification	SOL1	SOL3
Viscosity (Pa s)	0.22	0.51
DMTA <sup>a</sup>		
$T_{gs}$ (°C)	-41	-45
$T_{gh}$ (°C)	35	56
Tensile strength (MPa)	8.9	3.8
Initial modulus (MPa)	9.0	9.3
Elongation at break (%)	91	196
Overall solvent spot	14	13
Swelling in		
2-Butanone	Dissolved	Dissolved
2-Propanol	Dissolved	Dissolved
Water	25	20
DMF	Dissolved	Dissolved
Xylene	182	211

<sup>a</sup>  $T_{gs}$  and  $T_{gh}$  correspond to the glass transition temperatures of the soft and hard domains, respectively.

distribution of DMPA will vary from polymer chain to polymer chain. In the case of AQ1 (98%), it is likely that all the chains will contain at least one DMPA moiety due to its higher molecular weight, whereas in AQ2 (120%), a fair number of chains may be devoid of DMPA, and, thus, less surface is generated, resulting in the larger particle diameter.<sup>31</sup>

There is also a dramatic deterioration in the mechanical properties when comparing AQ1 with AQ2. GPC studies were unable to provide absolute values for the molecular weights of these samples. However, the trends expected from the theory of the chain extension process were evident. The results, shown in Table V, from the GPC analysis, confirm that AQ1 has a higher molecular weight than has AQ2. Hence, the results suggest that small differences in the molecular weight contribute as well as ionic and hydrogen bonding to the significant differences in the properties exhibited by the samples. Table IV includes the mechanical properties of the two waterborne samples, AQ1 and AQ2, carried out at 80°C. Comparing the tensile strength results with those at room temperature, a significant drop was observed for both samples. This decrease is attributable to the breakage of hydrogen bonds in the samples. However, the 98% chain-extended sample, AQ1, still had a much greater tensile strength than that of AQ2. This suggests that tensile strength is not solely a result of differing hydrogen-bond contents and ionic interactions, but that molecular weight

differences play an important role in the development of the mechanical properties and structure of the samples. It is unlikely that the ionic interactions also dissociate at 80°C and they continue to contribute to the tensile strength. Hence, for AQ2, it appears that very few of these ionic interactions occur and its mechanical properties are primarily governed by hydrogen bonding, probably a very minor contribution at 80°C, and molecular weight. The elongation was seen to increase with temperature for both water-borne samples. AQ2 exhibited a greater elongation than did AQ1, which is consistent with the latter having a higher number of ionic interactions as already suggested from their respective tensile strengths. These ionic interactions restrict the extensibility of the PU.

It also appears that as the chain-extension level is increased beyond a 1 : 1 NCO/NH<sub>2</sub> ratio the extent of phase separation decreases. Figure 5 shows clearly the increase in the degree of mixing of the hard and soft phases as the chain extension is increased from AQ1 to AQ2. The same was observed for the solvent-borne systems on comparing SOL1 and SOL2 of chain extension 120 and 150%, respectively. In Figure 6, DMTA experiments run in the shear mode for AQ1 and AQ2 are shown. The high-temperature transition (90°C in AQ1 and 45°C in AQ2) corresponds to the dissociation of the hard domains. This transition corresponds to the breakage of hydrogen bonds, but the presence of ionic interactions in AQ1 causes this transition to shift to a higher temperature. The transitions appearing above 100°C are associated with ionic dissociation or rearrangement.<sup>32</sup> Such ionic transitions have been previously observed by DMTA<sup>33</sup> and dielectric measurements.<sup>34</sup>

#### Effect of DMPA Incorporation into the Solvent-Borne PU Backbone

The compositions of SOL1 and SOL3 are outlined in Table I. SOL1 contained the carboxylic species which were neutralized with TEA. However, SOL3 had no DMPA incorporated into its backbone. The results from the characterization of these two samples are shown in Table VI. The presence of ionic groups incorporated into the hard segments of SOL1 had a significant effect on its tensile strength compared to SOL3. The carboxylate ions in SOL1 enhances phase separation through ion-hydrogen bonding which can be detected by IR spectroscopy. DMTA results suggest that the morphologies of SOL1 and 3 are very

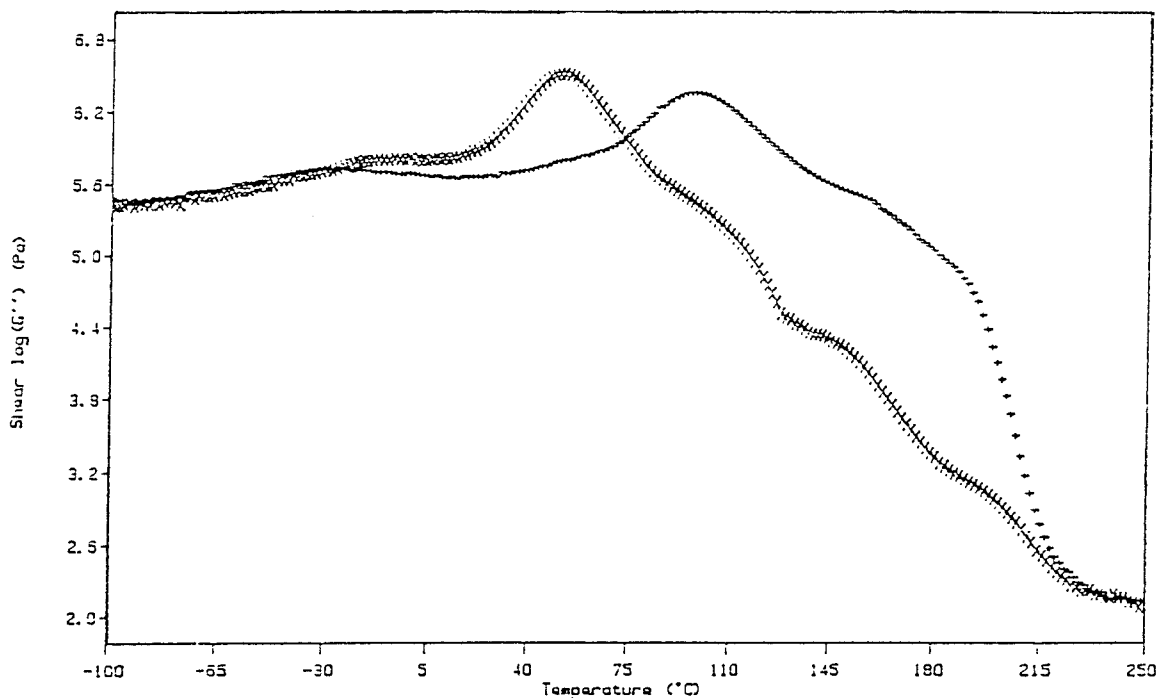


**Figure 6** Loss modulus vs. temperature plots of (+) AQ1 and (×) AQ2 of 98 and 120% chain extension, respectively. Conducted in the shear mode.

similar. However, hydrogen bonds formed with the carboxylate ion appear to be stronger than are hydrogen bonds between  $\text{—NH}$  and  $\text{C=O}$  groups because their tensile strengths are clearly different. In fact, these ion–hydrogen bonds are approximately 1.3 times<sup>35</sup> stronger than are ordinary hydrogen bonds. If there are sufficient numbers of the ionic groups present, a phase-separated structure is favored. However, at lower levels, these disrupt the hard-phase structure which can result in component mixing. In this case, the ionic groups are not present in sufficient numbers to alter the phase structure dramatically, but there are enough to enhance the tensile strength of the DMPA-containing SOL1 film.

From an examination of the infrared spectra of the samples (Fig. 7), it is noticeable that the  $\text{C—O—C}$  band of the soft segment at approximately  $1110\text{ cm}^{-1}$  is at a lower frequency for SOL3 than for SOL1. This phenomenon was described in the work by Chen.<sup>35</sup> He stated that for an un-ionized film the  $\text{—NH}$  groups can form hydrogen bonds with  $\text{C=O}$  of the hard segment and also with a  $\text{C—O—C}$  group of the soft segment. After ionization, some of the  $\text{—NH}$  groups previously bonded to the  $\text{C—O—C}$  groups shift to bond with the  $\text{C=O}$  groups of the hard segments. Hence, the number of hydrogen bonds between soft and

hard segments diminishes and this results in the  $\text{C—O—C}$  band shifting to a higher frequency. So, from this, one would expect significant hard–hard phase interactions in SOL1 and a rather more defined structure. The tensile strengths of the two samples shown in Table V certainly suggest this is the case. For SOL3, however, the infrared results suggest that there are a higher number hard–soft phase interactions than for SOL1. This will contribute to its lower tensile strength as well as to its less phase-separated structure.

#### Examination of Crystallinity

The crystallinity of all the samples used in this study were investigated using DSC and WAXD. It was determined that no significant crystallinity existed in any of the samples, and, hence, no account of crystallinity was required in order to explain the structure and property differences of the samples. A single diffuse peak was obtained for all samples from WAXD, which is expected for amorphous materials. The findings from these investigations suggest that the soft segment is of insufficient length to crystallize and the unsymmetrical nature of the diisocyanate is unlikely to form hard-segment crystallites.



3. D. Dieterich, *Angew. Chem. Int. Eng. Ed.*, **9**, 40 (1970).
4. K. Matsuda, *J. Appl. Polym. Sci.*, **23**, 141 (1979).
5. P. H. Markusch, U.S. Pat. 4,408,008 (1983).
6. H. Hsieh, U.S. Pat. 4,237,246 (1980).
7. P. H. Markusch, U.S. Pat. 4,238,378 (1980).
8. K. C. Frisch and D. Klempner, Eds., *Adv. Urethane Sci. Technol.*, **10**, 121 (1987).
9. R. Buscall, T. Corner, and J. F. Stageman, *Polymer Colloids*, Elsevier, New York, 1985.
10. G. Oertel, *Polyurethane Handbook*, 2nd ed., Carl Hanser Verlag, Munich, 1993.
11. C. Geraldine and A. Eisenberg, *Ind. Eng. Chem. Prod. Res. Dev.*, **20**, 271 (1981).
12. O. Lorenz, H. J. August, H. Hick, and F. Triebes, *Angew. Makromol. Chem.*, **63**(1), 11 (1977).
13. O. Lorenz and H. Hugo, *Angew. Makromol. Chem.*, **72**, 115 (1978).
14. D. Dieterich, G. Balle, and H. Schmeiner, *Ger. Offen.*, 2,735,013 (1979).
15. Z. Wirpsza, *Polyurethanes: Chemistry, Technology & Applications*, Polymer Science Series, Ellis Horwood, New York, 1993.
16. Y. S. Ding, *Polymer*, **30**, 1204 (1989).
17. N. L. Brockman, *J. Polym. Sci. Polym. Phys. Ed.*, **23**, 1145 (1985).
18. D. J. Yarusso, *Macromolecules*, **16**, 1871 (1983).
19. M. Gauthier, *Macromolecules*, **22**, 3754 (1989).
20. M. Gauthier, *Macromolecules*, **23**, 2066 (1990).
21. R. A. Register, *Macromolecules*, **21**, 1009 (1988).
22. B. Broze, *Macromolecules*, **16**, 996 (1983).
23. D. J. Yarusso, *J. Polym. Sci. Phys. Ed.*, **22**, 2073 (1984).
24. D. J. David and H. B. Staley, *Analytical Chemistry of Polyurethanes*, High Polymer Series, Part 3, Wiley-Interscience, New York, 1969.
25. T. Schatzki, *J. Polym. Sci.*, **57**, 496 (1962).
26. J. A. Sauer, *J. Polym. Sci.*, **57**, 497 (1962).
27. F. P. Reding, *J. Polym. Sci.*, **57**, 496 (1962).
28. C. K. Kim and B. K. Kim, *J. Appl. Polym. Sci.*, **43**, 2295 (1991).
29. K. Knutson and D. J. Lyman, *Adv. Chem. Ser.*, **199**, 109(1982).
30. Y. M. Lee, J. C. Lee, and B. K. Kim, *Polymer*, **35**(5), 1095 (1994).
31. B. K. Kim and T. K. Kim, *J. Appl. Polym. Sci.*, **43**, 393 (1991).
32. S. A. Visser and S. L. Cooper, *Macromolecules*, **24**, 2576 (1991).
33. W. J. MacKnight, L. W. McKenna, and B. E. Read, *J. Appl. Phys.*, **38**, 4208 (1967).
34. B. E. Read, E. A. Carter, T. M. Connor, and W. J. MacKnight, *Br. Polym. J.*, **1**, 123 (1969).
35. S.-A. Chen and J.-S. Hsu, *Polymer*, **34**(13), 2769 (1993).